High channel-count phase-only sampled fiber Bragg grating and its application to dispersion compensator and multi-wavelength fiber laser

Hongpu Li

Department of Electrical and Electronic Engineering, Shizuoka University,
Johoku 3-5-1,Hamamatsu, 432-8561, Japan
*dhli@ipc.shizuoka.ac.jp

ABSTRACT

In this paper, we introduce our recent developments in the design techniques for high channel-count fiber Bragg gratings (FBG). Based on a double sampling method, we theoretically demonstrate a linearly chirped FBG with channels up to 153, which could be used as the dispersion compensator. Moreover, we propose a novel technique for the realization of a multi-channel notch filter by using a thermally-induced phase-shift of this kind of FBG. As an example, a multi-channel narrow band-pass filter is realized and successfully used to implement a multi-wavelength fiber laser.

Keywords: Fiber Bragg grating (FBG), phase-only sampling, wavelength-division multiplexing (WDM), dispersion and dispersion slope compensator, phase shifted FBG, multichannel notch filter, multi-wavelength fiber laser.

1. INTRODUCTION

High channel-count fiber Bragg grating has recently attracted great interests due to its excellent channel performances for wavelength filtering used as either chromatic dispersion compensators, or comb filters for multi-wavelength fiber laser sources, or the dispersive components for the generation of high-repetition-rate pulse sequences [1]-[16]. However, with increasing the number of wavelength-division-multiplex (WDM) channels to cover the full S-, C-, or L-band, high channel-count FBG device becomes extremely difficult to realize due to the requirements of a considerably high index-modulation and the tremendous precision of the FBG writing tools. In this paper, we review our recent developments in the design and fabrication techniques for high channel-count fiber Bragg gratings (FBG). We have theoretically demonstrated a novel double sampled FBG with channels up to 153, which could be used as a dispersion compensator. Moreover, we propose a novel technique for the realization of a multi-channel notch filter by using a thermally-induced phase-shift of this kind of FBG. Besides its intrinsic properties including a continuously tuning range, easy control, low cost, narrow bandwidth, and low polarization sensitivity, this technique offers one unique advantage of multi-channel response simultaneously by controlling the phase-shift at one-point. As an example, based on the utilization of two concatenated FBGs (one of them is phase-shift inserted), a multi-channel narrow band-pass filter is obtained and successfully used to implement a multi-wavelength fiber laser.

2. ULTRAHIGH CHANNEL-COUNT DUAL-AMPLITUDE-ASSISTED PHASE-ONLY SAMPLED FBG COVERING THE S, C, AND L BANDS

Multi-channel FBGs with the channel count 51, used as either the dispersion compensator or the simultaneous dispersion and dispersion slope compensator, have already been demonstrated, in which a continuous phase-only sampling function with excellent channel uniformity and high in-band energy efficiency is utilized[9, 17]. The sampling function proposed can be optimally obtained by using either the simulated annealing algorithm or the other nonlinear optimization methods such as the downhill and the gradient-descent optimization method. However, with further increasing the number of wavelength-division-multiplex (WDM) channels (e.g.,～120) to cover through the S-, C- and L-band simultaneously, optimization for the phase-only sampling function becomes extremely difficult or even impossible to be realized by

Photonics and Optoelectronics Meetings (POEM) 2009: Optoelectronic Devices and Integration,
edited by Zishen Zhao, Ray Chen, Yong Chen, Jinzhong Yu, Junqiang Sun, Proc. of SPIE
Vol. 7516, 751608 · © 2009 SPIE · CCC code: 0277-786X/09/$18 · doi: 10.1117/12.837335

using the current nonlinear algorithms, because too large number of the free-parameters need to be optimally decided, which thus makes the phase-only sampled FBGs with channel count above 100 rarely being studied and reported. In the following parts, a novel double sampling scheme enabling to create an ultrahigh channel-count FBG with excellent channel uniformity and high in-band energy efficiency is firstly proposed.

2.1 Principle of the double sampling method

Unlike the traditional sampled FBG, a double sampled FBG is the product of a single-channel seed grating Δn_{sg} with two sampling functions $s_1(z)$ and $s_2(z)$. The induced refractive index-modulation $\Delta n_s(z)$ can be expressed as [18]

$$\Delta n_s(z) = \mathrm{Re}\{\Delta n_{sg}(z)\cdot s_1(z)\cdot s_2(z)\} = \mathrm{Re}\left\{\frac{\Delta n_1(z)}{2}\exp\left[i\frac{2\pi z}{\Lambda} + i\phi_g(z)\right]\cdot s_1(z)\cdot s_2(z)\right\}. \quad (1)$$

Here $\Delta n_1(z)$ is the maximum index-modulation of the seed grating, z is the position along the grating, Λ represents the average uniform period of the seeding grating, $\phi_g(z)$ denotes the phase-change related to the chirp properties of the seed grating. For convenience, the "dc" part of the index-modulation is neglected in Eq. (1). In our case, $s_1(z)$ is assumed to be an amplitude-assisted phase-only sampling function (AAPS), and meanwhile $s_2(z)$ is assumed to be a phase-only sampling function (POS) which can be expressed as

$$s_1(z) = a_1(z)\cdot \exp[i\theta_1(z)] = \sum_{m=-\infty}^{\infty} S_{1m}\exp[i2m\pi z/P_1], \quad (2)$$

$$s_2(z) = \exp[i\theta_2(z)] = \sum_{m=-\infty}^{\infty} S_{2m}\exp[i2m\pi z/P_2], \quad (3)$$

where $\alpha_1(z)$ and $\theta_1(z)$ denote the amplitude and phase distribution of the function $s_1(z)$, and $\theta_2(z)$ denotes the phase distribution of the POS function $s_2(z)$. The summation terms in Eqs. (2) and (3) denotes the sampling functions expanded in Fourier series, respectively, where P_1 and P_2 are the periods of the sampling functions and the in-band channels considered are assumed to be $2N_1+1$ and $2N_2+1$, respectively. The channel spacings $\Delta\nu_1$ and $\Delta\nu_2$ (in frequency domain) are given as $\Delta\nu_1 = c/2n_{eff}P_1$ and $\Delta\nu_2 = c/2n_{eff}P_2$, respectively. S_{1m} and S_{2m} are the complex Fourier coefficients, n_{eff} is the effective index of FBG and c is the velocity of light in vacuum. By using the simulated annealing algorithm and Gerchberg-Saxton iterative method [7, 19], this sampling functions $s_1(z)$ is optimized so that the absolute value of the Fourier coefficients are identical within the band of interest and the other Fourier coefficients beyond $|m| \le N_1$ are zero. Meanwhile the magnitude of $|\alpha_1(z)|$ near to a unit is compulsively demanded. Once the sampling function $s_1(z)$ is optimally established, the Eq. (2) can be rewritten as

$$s_1(z) = \sum_{m=-N_1}^{N_1} S_{1m}\exp(i2\pi mz/P_1). \quad (4)$$

For the phase-only sampling function $s_2(z)$ with in-band channels $2N_2+1$, it can be obtained by using the same method what we described and used in [7]. However, since it is phase-only one, the out-band channel cannot be eliminated. Figure 1 shows the principle of the double sampling function (AAPS+POS) based on the Fourier theory. Figure 1(d) shows the reflection spectrum of the realized FBG using the double sampling method (AAPS+POS), it can be seen that one can easily obtain consecutive $(2N_1+1)\cdot(2N_2+1)$ channels with a channel spacing of $\Delta\nu_1$ in the frequency domain. Therefore, the channel number can be easily and considerably increased. To avoid overlapping among the generated channels, the condition $P_2 \le P_1/(2N_1+1)$ should be satisfied.

2.2 Design results utilizing the double sampling method: (AAPS + POS)

To verify the above proposal, the typical design for the FBG with consecutive 135 channels is implemented. Firstly, an AAPS function with 3-channel and a POS function with 45-channel are designed [20]. To guarantee the in-band energy (diffraction) efficiency of 100%, there generally exists a small and low-frequency oscillation on the amplitude profile of the 3-channel sampling function. For higher channel-count phase-only sampling function of (45 in our case), the non-uniformity over all 45 channels is less than 0.5% and the in-band energy (diffraction) efficiency is larger than 93%. The sampling period of the 3-channel sampling function is 1 mm (i.e., the channel spacing is 0.8 nm). To satisfy the condition $P_2 \le P_1/(2N_1+1)$, the sampling period of the 45-channel sampling functions is chosen as 1/3 mm (i.e., the channel spacing is 2.4 nm for wavelength at 1550 nm). Secondly, a seed grating is designed by using the layer peeling method [21]. The seed grating is designed to have the chromatic dispersion compensation of -1360 ps/nm, a length of 12 cm, and the 0.5-dB bandwidth of 0.4 nm. By multiplying the seed grating with the 3- and 45-channel sampling functions in spatial domain, an ultrahigh channel-count FBG with 45 sets of 3-channel (i.e., 135 consecutive channels) is realized. The design results of the 135-channel double sampled FBG (AAPS+POS) are illustrated in Fig. 2. Figure 2(a) shows the index-modulation profile, the inset shows the fine profile within 1mm region in the grating direction. It can be seen that the maximum index-modulation is less than 8×10^{-4}, which is easily obtainable with the current hydrogen-loaded photosensitive fiber. There also exists a cosine-like oscillation on the grating profile, period of which is about 0.5 mm, which is determined by the 3-channel AAPS function. By using the advanced phase-mask writing technique incorporated with a narrow writing beam [9], it is possible for one to write this kinds of low-frequency oscillation on the envelop of the FBG. The calculated reflection and group delay spectra of the 135-channel FBG covering a wavelength range of 108 nm are shown in Fig. 2(c). To illustrate the spectra clearly, three channels locating at the central wavelengths of 1509 nm, 1545 nm, and 1581 nm are given in the insets of Fig. 2(c). Moreover, the group delay ripples for all in-band channels are smaller than ±1 ps.

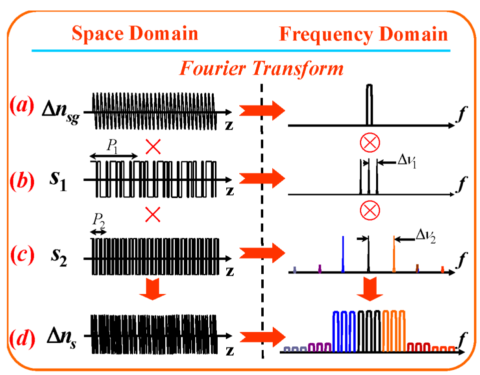

Fig. 1. Fourier analysis of the proposed double sampling method for the design of ultrahigh-channel-count, ultra-broadband FBG.

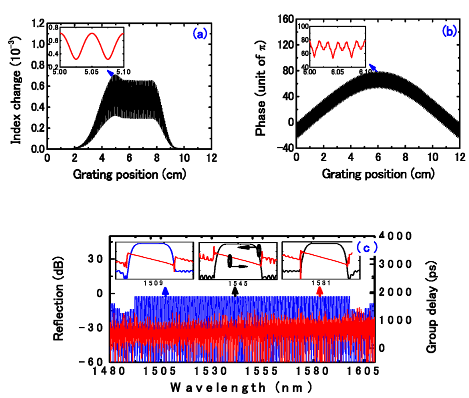

Fig. 2. Design results for a 135-channel double sampled FBG (AAPS+POS). (a) grating index profile, the inset shows the fine index profile within a region of 1mm, (b) grating phase profile,

the inset shows the fine phase profile within a region of 1mm, (b) reflection and group delay spectra, the insets show the spectra at the wavelengths of 1509 nm, 1545 nm and 1581 nm, respectively.

3. MULTI-CHANNEL NOTCH FILTER BASED ON THE PHASE-SHIFTED PHASE-ONLY-SAMPLED FBG AND ITS APPLICATION TO MULTI-WAVELENGTH FIBER LASER

3.1 Multi-channel notch filter based on a phase-shifted phase-only-sampled fiber Bragg grating

As a phase shift θ is introduced in the sampled FBG at the position of z_0 , the index modulation can be equivalently written as[22]

$$\Delta n'(z) = \begin{cases} \mathrm{Re}\left\{\left[\Delta n_0 + \frac{\Delta n_1(z)}{2}\cdot \exp\left(i\frac{2\pi z}{\Lambda(z)}\right)\right]\cdot s(z)\right\} & \text{when } z \le z_0 \\ \mathrm{Re}\left\{\left[\Delta n_0 + \frac{\Delta n_1(z)}{2}\cdot \exp\left(i\frac{2\pi z}{\Lambda(z)}\right)\right]\cdot \exp(i\theta)\cdot s(z)\right\} & \text{when } z > z_0 \end{cases}. \tag{5}$$

It is obviously seen from Eq. 5 that the phase-shift phase-only sampled FBG is equivalent to a phase-shift single channel FBG (also called the seed grating) multiplied by a sampling function in spatial domain. Therefore, the reflection spectrum resulted from a phase-shifted seed grating should be copied simultaneously through all the sampled channels.

3.2 Experimental results for the notch filter

The schematic diagram of the proposed multi-channel notch filter is shown in Fig. 3, where the phase-only sampled FBG is vertically placed on a NiCr wire heater which is fixed in a V-groove. The V-groove is fabricated on a heat-insulating material. Because of the thermo-optical effect, the refractive index of the fiber will change with the temperature of the wire heater (i.e., NiCr wire, its diameter is about 0.3mm). Hence, the temperature change in a local small section of the fiber will introduce a phase shift at that point. An amplified spontaneous emission (ASE) is used as the broadband light source (BLS). As shown in Fig. 3, a simple circuit including a variable resistor and a direct current source is employed to control the temperature of the NiCr wire. A heat sink made from a thin copper plank is placed over the crossing area to dissipate the unwanted heat. A linearly chirped phase-only sampled 51-channel FBG with channel bandwidth of 0.6 and spacing of 0.8 nm has been employed here [9]. Figure 4 shows the experimental measurement for the reflection spectrum, it is seen that the characteristics are almost the same with the designed one used in the above section. By carefully adjusting the variable resistor, the minimum bandwidth of the notch filter can be obtained in the reflection spectrum which should be related to the phase shift. Figure 4 shows the reflection spectrum of the 51-channel FBG with π phase shift, which is measured by using optical spectrum analyzer (OSA). The reflection spectrum of central three channels is shown in Fig. 4(b). The FWHM of the notch filter is about 0.026 nm at the central channel which agrees well with the numerical results in the above section.

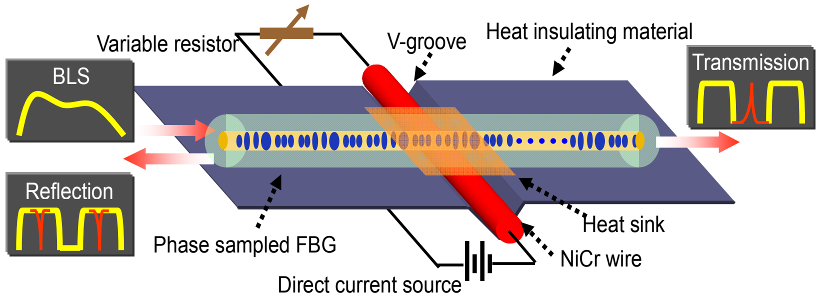

Fig. 3. Schematic diagram of the proposed multi-channel notch filter: Broadband light source (BLS).

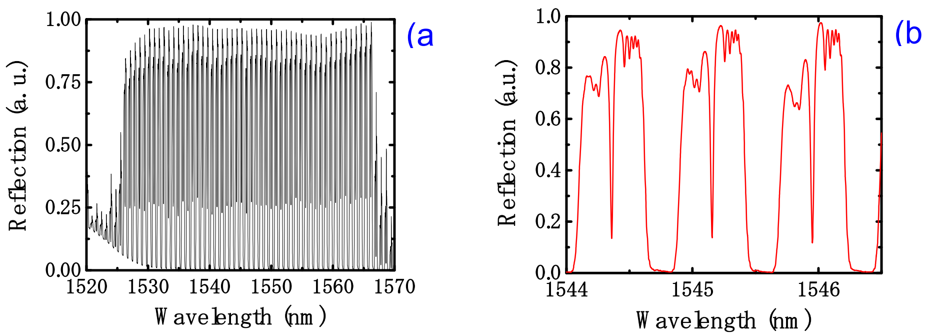

Fig. 4. Measurement results for the π phase shifted 51-channel FBG. (a) Reflection spectrum, and (b) reflection spectrum of the central three channels.

3.3 Optical semiconductor amplifier based multi-wavelength fiber laser

Figure 5 shows the schematic diagram of the experimental setup for the multi-wavelength fiber laser. This setup consists of a SOA (with a maximum small-signal gain of 19 dB and a polarization dependent gain of 0.7 dB), two isolators, one polarization controller (PC), one 10/90 power coupler, one circulator, and two concatenated 51-channel linearly-chirped FBGs. This two gratings are particularly designed and have been used as a dispersion compensator in fiber link system [19], which have identical characteristics with a channel bandwidth (1-dB) of 0.6 nm and channel spacing 0.8 nm. The reason for choosing such a linearly-chirped FBG lies on those: firstly, it can provide a relative wide bandwidth (0.4-0.6 nm) in each channel. Secondly, the notch wavelength resulted from the thermally induced phase-shift in the FBG has a linear relationship with the grating position where the phase-shift is inserted, which in return means that tunability of the notch wavelength is easily realized. Third, it can provide one a very precise and a fixed channel-spacing, which is exactly fitted with ITU channel grids. The inset of Fig. 5 shows schematic diagram of the multiple phase-shifts phase-only sampled FBG, where several NiCr wires (heaters) located in the V-grooves are employed to inscribe multiple phase-shifts in the FBG based on the thermal-optical and thermal-expansion effect. In particular, three NiCr wires labeled as #1, #2 and #3 are employed in this setup. By switching any either one or two of the driving circuits simultaneously and tuning the corresponding variable resistors, one or two π phase-shifts can be inserted at the grating positions where the NiCr wires are located. Moreover, the separation between the two phase-shifts resulted could be easily changed in steps either by heating the different two NiCr wires or by changing the separation of the paired two-wires mechanically. To make the noth filters thermally stable, two heat sinks made from a thin copper plank are utilized and respectively placed over the regions where the V-grooves and NiCr wires lie in.

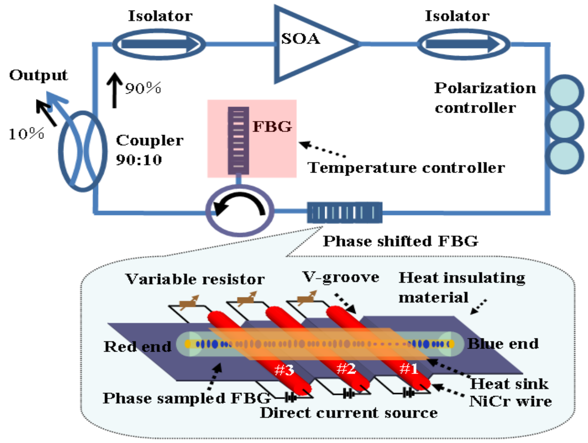

Fig. 5. Experimental setup for lasing wavelength multiplication of SOA-based fiber ring laser, the inset illustrates the schematic diagram of the multiple phase-shifts phase-only sampled FBG.

Once a π phase shift is introduced into the phase-only sampled FBG, 51 notch filters will be generated simultaneously. One of the gratings, i.e., the one without the phase-shift inserted, is placed in a temperature controlling chamber. When the reflection spectrum is appropriately shifted in accordance to the phase shifted FBG, the output spectrum of the two concatenated FBGs is exactly functioned as a multi-channel narrow band-pass filter [22]. Figure 6(a) shows the output spectrum of the proposed laser scheme working at room temperature, which is obtained by using an optical spectrum analyzer with a wavelength resolution of 0.01nm. The operating current of the SOA is 250 mA. For reference, the small-signal gain spectrum of the OSA is measured and given in the inset of Fig. 6(a). It is seen that more than 30 wavelengths (within a variation of 7.4 dB) lasing with an identical channel spacing 0.8 nm have been obtained. The signal-to-noise ratio is above 50 dB as shown in Fig. 6(b). Once two π phase shifts are simultaneously introduced into the phase-only sampled FBG, a 51-channel dual-bandpass filter can be generated in the transmission spectrum of the two concatenated FBGs. Figure 7 shows the output spectrum of the proposed fiber laser working at room temperature, which is obtained by using an optical spectrum analyzer with a wavelength resolution of 0.01nm. Figure 7(b) shows the spectrum of one typical dual-wavelength lasing in Fig. 7(a). It is seen that more than 20 dual-wavelength lasing with the channel spacing of 0.8 nm have been obtained. The signal-to-noise ratio (SNR) and the 3-dB linewidth of the dual-wavelength lasing are higher than 45 dB, and less than 0.0155 nm, respectively, which are difficult to be realized in the general SOA-based fiber ring laser. Moreover, the obtained fiber laser has a fixed spacing of 0.8 nm between each dual-wavelength which makes it exactly compatible with the standard ITU grids and thus easier to be integrated into the commercial WDM system. It must be noted that the lasing linewidth shown in Fig. 6(b) and Fig. 7 (b) are roughly estimated and limited by the resolution of the available OSA (10 pm). Moreover, the resulted bandwidth ~0.026 nm (~3 GHz) of the obtained band-pass filter (as is shown in Fig. 4(b)) is not small enough to make the multiple single- and dual-wavelength lasing at single-longitude-mode (SLM). The probable approaches to further decrease the lasing linewidths may be the ones by either considerably increasing the strength of the FBG, or decreasing the length of the fiber ring (cavity), or doing the above both simultaneously [23].

Next, to investigate the spectral stability of the proposed laser, we repeatedly measure the output spectrum of all the multiple dual-wavelength lasing by scanning the optical spectrum analyzer 11 times in every other 5 minute. Figure 8(a) shows the ten spectra ranges from 1530 nm to 1570 nm, where a good stability in the inter-channel output has been clearly exhibited. The maximum variation of the peak output power for the dual-wavelength lasing is less than 2 dB which is mainly caused by the non-uniform heat-dissipation of two NiCr wires. So that a more effective heat sink to rapidly eliminate the heat diffusions may be helpful to reduce the maximum power variation. Figure 8(b) shows the output spectra of the two typical dual-wavelength lasings, which correspond to the cases where the #2 & #3 (separation is 1.5 cm) wires and #1 & #3 NiCr wires (separation is 3.0 cm) are heated, respectively. Since the length of the linearly chirped phase-only sampled FBG used is 12 cm and the bandwidth of each channel is 0.6 nm, a separation of 1.5 and 3 cm for the π phase shifts inserted will be accordingly related to a wavelength interval of 0.075 nm, and 0.15 nm, respectively. The wavelength spacing of the paired dual-wavelength lasing shown in Fig. 8(b) is about 0.075 and 0.145 nm, respectively, which agree wells with what we expect. The results shown in Fig. 8(b) mean that wavelength spacing within each dual-wavelengths may be tunable. It is expected that a multiple triplex- or quadruple-wavelength of this kind of fiber laser can also be implemented if more discrete phase shifts are introduced [24].

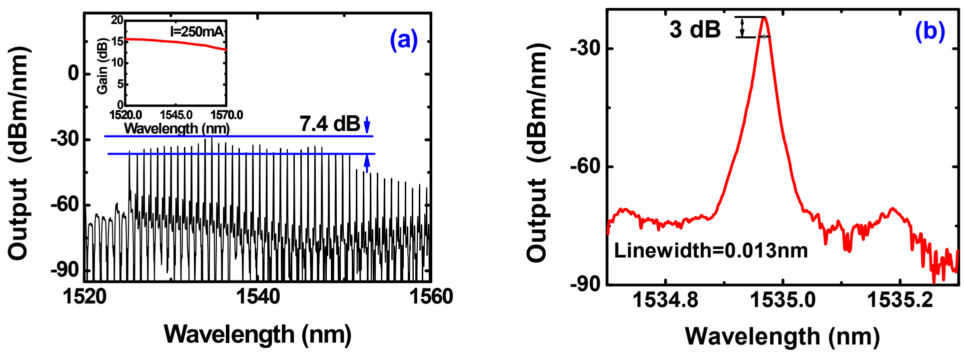

Fig. 6. (a) Output spectrum of the SOA-based multi-wavelengths SOA-based fiber ring laser, and (b) spectrum of Fig. 7(a) for typical wavelength lasing.

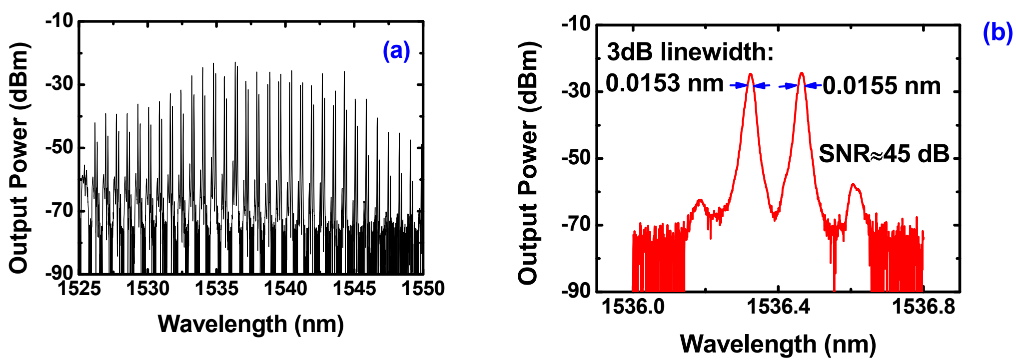

Fig. 7. (a) Output spectrum of the SOA-based multiple dual-wavelengths SOA-based fiber ring laser, and (b) spectrum of Fig. 8(a) for typical dual-wavelength lasing.

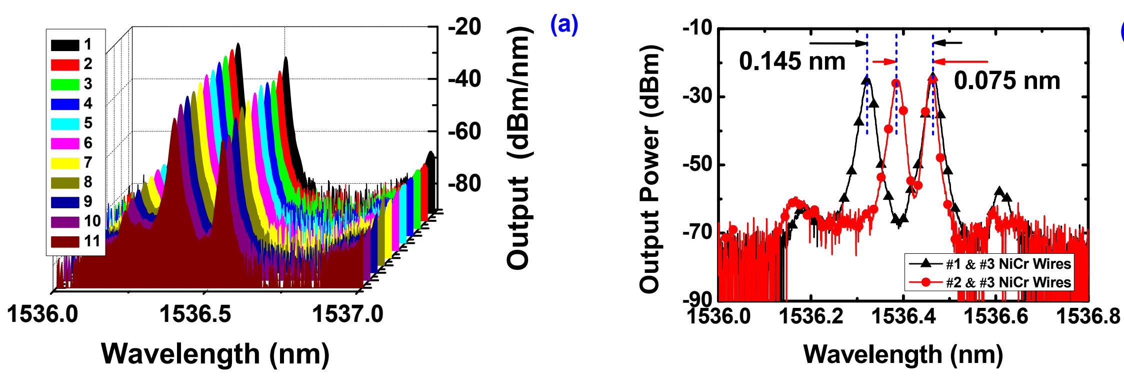

Fig. 8. (a) Eleven output power spectra of typical dual-wavelength lasing with a time interval of 5 minutes, and (b) output power spectra of typical dual-wavelength lasing with two different distances of 1.5 cm and 3 cm, respectively.

4. ONCLUSION

In this paper, a novel double sampling scheme enabling to create an ultrahigh channel-count fiber Bragg grating (FBG) with excellent channel uniformity and high in-band energy efficiency is proposed, which is based on the simultaneous utilization of two phase-only sampling functions. With this method, a linearly chirped 135-channel FBG with a length of 12 cm, a dispersion of 1360 ps/nm, channel spacing of 0.8 nm, and grating strength of 10 dB is theoretically demonstrated and the maximum refractive index- change required is less than 10^{-3}. Moreover, we propose a novel technique for the realization of a multi-channel notch filter by using a thermally-induced phase-shift of multi-channel FBG. Besides its intrinsic properties including a continuously tuning range, easy control, low cost, narrow bandwidth, and low polarization sensitivity, this technique offers one unique advantage of multi-channel response simultaneously by controlling the phase-shift at one-point. As an example, based on the utilization of two concatenated FBGs (one of them is phase-shift inserted), a multi-channel narrow band-pass filter is obtained and successfully used to implement a multi-wavelength fiber laser.

ACKNOWLEDGEMENTS

This work was partly supported by Kurata Memorial Hitachi Science and Technology Foundation, the International Communications Foundation, and Hamamatsu Science and Technology Promotion in Japan. The authors would like to thank Dr. Yves Painchaud of TeraXion Inc. for his kindly help. Dr. Ming Li is also acknowledged for his contributions when he studied in Shizuoka University.

REFERENCES

[1] B. Eggleton, P. A. Krug, L. Poladian, and F. Oullette, “Long periodic superstructure Bragg gratings in optical fibres,” Electron. Lett. 30(19),1620-1622 (1994).

[2] F. Oullette, P. A. Krug, T. Stephens, G. Dhosi, and B. Eggleton, “Broadband and WDM dispersion compensation using chirped sampled fibre Bragg gratings,” Electron. Lett. 31(11), 899-901 (1995).

[3] M. Ibsen, M. K. Durkin, M. J. Cole, and R. I. Laming, “Sinc-sampled fiber Bragg gratings for identical multiple wavelength operation,” IEEE Photon. Technol. Lett. 10(6), 842-844 (1998).

[4] W. H. Loh, F. Q. Zhou, and J. J. Pan, “Sampled fiber grating based-dispersion slope compensator,” IEEE Photon. Technol. Lett. 11(10), 1280-1282 (1999).

[5] A.V. Buryak, K.Y. Kolossovski, K.Y.Stepanov and D. Yu, “Optimization of refractive index sampling for multichannel fiber Bragg gratings,” IEEE J. Quantum Eelctron. 39(9), 91-98 (2003).

[6] J. E. Rothenberg, H. Li, Y. Li, J. Popelek, Y. Wang, R. B. Wilcox, and J. Zweiback, “Dammann fiber Bragg gratings and phase-only sampling for high channel counts,” IEEE Photon. Technol. Lett. 14(9),1309-1311 (2002).

[7] H. Li, Y. Sheng, Y. Li, J. E. Rothenberg, “Phased-only sampled fiber Bragg gratings for high channel counts chromatic dispersion compensation,” J. Lightwave Technol. 21(9), 2074-2083 (2003).

[8] Y. Painchaud, A. Mailoux, H. Chotard, E. Pelletier, and M. Guy, “Multi-channel fiber Bragg gratings for dispersion and slope compensation,” in Proc. Optical Fiber Communication Conference (Optical Society of America, Washington, D.C., 2002), paper ThAA5.

[9] M. Morin, M. Poulin, A. Mailloux, F. Trépanier and Y. Painchaud, “Full C-band slope-matched dispersion compensation based on a phase sampled Bragg grating,” Proceedings of OFC04, Paper WK1 (2004).

[10] H. Li, M. Li, K. Ogusu, Y. Sheng, and J. E. Rothenberg, “Optimization of a continuous phase-only sampling for high channel-count fiber Bragg gratings,” Opt. Express 14(8),3152 – 3160 (2006).

[11] H. Li, M. Li, Y. Sheng, and J. E. Rothenberg, “Advances in the design and fabrication of high channel-count fiber Bragg gratings,” IEEE J. Lightwave Technol., 25(9), 2739-2749 (2007).

[12] H. Lee and G. Agrawal, “Bandwidth equalization of purely phase-sampled fiber Bragg gratings for broadband dispersion and dispersion slope compensation,” Opt. Express 12(23), 5595-5602 (2004).

[13] A. Bellemare, M. Karasek, M. Rochette, S. LaRochelle, and M. Tetu, “Room temperature multifrequency Erbium-doped fiber lasers anchored on the ITU frequency grid,” IEEE J. Lightwave Technol. 18(6), 825-830 (2000).

[14] J. Magne, P. Giaccari, S. LaRochelle, J. Azana, L. R. Chen, “All-fiber comb filter with tunable free spectral range,” Opt. Lett. 30(16), 2062-2064 (2005).

[15] P. Petropoulos, M. Ibsen, M. N. Zervas, and D. J. Richardson, "Generation of a 40-GHz pulse stream by pulse multiplication with a sampled fiber Bragg grating," Opt. Lett. 25(8), 521-523 (2000).

[16] J. Azana, R. Slavik, P. Kockaert, L. R. Chen, S. LaRochelle, "Gereration of customized ultrahigh repetition rate pulse sequences using superimposed fiber Bragg gratings," IEEE J. Lightwave Technol. 21(6), 1490-1498 (2003).

[17] M. Li and H. Li, "Reflection equalization of the simultaneous dispersion and dispersion-slope compensator based on a phase-only sampled fiber Bragg grating," Optics Express 16 (13), 9821-9828 (2008).

[18] H. Li, M. Li, and J. Hayashi, "Ultrahigh channel-count phase-only sampled fiber Bragg grating covering the S-, C- and L-band," *Opt. Lett.* 34 (7), 938-940 (2009).

[19] R. W. Gerchberg and W. O. Saxton,"A practical algorithm for the determination of phase from image and diffraction image and diffraction plane pictures," Optik **35**, 237–246 (1972).

[20] M. Li, X. Chen, J. Hayashi, and H. Li, "Advanced design of the ultrahigh-channel-count fiber Bragg grating based on the double sampling method," Opt. Express 17(10), 8382-8394 (2009).

[21] J. Skaar, L. Wang, and T. Erdogen, "On the synthesis of fiber Bragg grating by layer peeling," IEEE J. Quantum. Electron., 37(2) 165-173 (2001).

[22] M. Li, H. Li, and Y. Painchaud, "Multi-channel notch filter based on a phase-shift phase-only sampled fiber Bragg grating," Opt. Express 16 (23), 19388-19394 (2008).

[23] M. Li, X. Chen, T. Fujii, Y. Kudo, H. Li, and Y. Painchaud, "Multiwavelength fiber laser based on the utilization of a phase-shifted phase-only sampled fiber Bragg grating," *Opt. Lett.* 34 (11), 1717-1719 (2009).

[24] M. Li, T. Fujii, H. Li, "Multiplication of a multi-channel notch filter based on a phase shifted phase-only sampled fiber Bragg grating," IEEE Photon. Technol. Lett. (2009) In Press.